

## Optical properties of the chalcopyrite semiconductors $\text{ZnGeP}_2$ , $\text{ZnGeAs}_2$ , $\text{CuGaS}_2$ , $\text{CuAlS}_2$ , $\text{CuInSe}_2$ , and $\text{AgInSe}_2$

J. C. Rife\* and R. N. Dexter

*University of Wisconsin, Madison, Wisconsin 53706*

P. M. Bridenbaugh

*Bell Telephone Laboratory, Holmdel, New Jersey 07733*

B. W. Veal

*Argonne National Laboratory, Argonne, Illinois 60439*

(Received 17 June 1977)

The reflectivities at 80 K of the chalcopyrite semiconductors  $\text{CuGaS}_2$ ,  $\text{CuAlS}_2$ ,  $\text{CuInSe}_2$ ,  $\text{AgInSe}_2$ ,  $\text{ZnGeP}_2$ , and  $\text{ZnGeAs}_2$  were measured in the energy range from 2 to 26 eV using synchrotron radiation. Occupied and unoccupied electronic states are described with the aid of the sharp reflectivity features from  $d$  levels and of the electronic spectrum from an ESCA spectrometer.

### I. INTRODUCTION

The II-IV- $V_2$  and I-III- $VI_2$  chalcopyrite semiconductors are of considerable interest as useful analogs of the III-V and II-VI semiconductors. They and their potential applications have been recently reviewed by Shay and Wernick.<sup>1</sup> Shileika<sup>2</sup> has also reviewed some properties of II-IV- $V_2$  semiconductors. We have measured the near-normal-incidence reflectivity of several ternary chalcopyrites for photon energies of 2–26 eV. Our measurements were primarily made at liquid-nitrogen temperatures in ultrahigh vacuum using the polarized and intense ultraviolet spectrum at the Wisconsin Synchrotron Radiation Center. We have studied  $\text{ZnGeP}_2$ ,  $\text{ZnGeAs}_2$ ,  $\text{CuGaS}_2$ ,  $\text{CuAlS}_2$ ,  $\text{CuInSe}_2$ , and  $\text{AgInSe}_2$  and have analyzed the broad-range optical properties in terms of electronic band structure. This analysis is made more plausible when reflectivity experiments are combined with x-ray photoemission spectroscopic (XPS) determinations of core levels and valence-band densities of states. XPS measurements were made by one of us, (B.W.V.), at the Argonne National Laboratory on specimens of  $\text{CuGaS}_2$ ,  $\text{CuAlS}_2$ ,  $\text{CuInSe}_2$ , and  $\text{ZnGeAs}_2$ .

In this paper we present the experimental results of XPS and reflectivity measurements and identify flat regions of  $p$ -like symmetry in the conduction band by utilizing reflectivity features associated with  $d$  and  $s$  core levels. We further show that these conduction-band states are the final states for critical transitions from other core or valence states which can be identified with the XPS spectrum. In only a few cases in this paper will we be able to confidently identify states in the chalcopyrite symmetry group or within the Brillouin zone.

In Sec. II we comment briefly on the chalcopyrite lattice and band structure. In Sec. III we outline the experimental procedure and the use of XPS data. In Sec. IV we present and discuss the results.

### II. TERNARY CHALCOPRITE SYSTEM

The following brief description is derived from Shay and Wernick.<sup>1</sup> The  $ABC_2$  chalcopyrite semiconductors take the zinc-blende structure with cations alternating on the lattice in a manner which leads to doubling of the length of the unit cell along the  $z$  direction ( $c$  axis). The differing electronegativities of cations  $A$  and  $B$  lead to a compression of the lattice and a crystalline field which is directly proportional to  $2 - c/a$ . A third anisotropy is a tetragonal distortion resulting from the displacement of the anion towards the  $A$  or  $B$  cation. The I-III- $VI_2$  chalcopyrites differ from the II-IV- $V_2$  chalcopyrites not only in being more ionic, and so with typically larger energy band gaps, but also because they contain  $d$  levels (from the I cations) which overlap the valence band. All of the I-III- $VI_2$  chalcopyrites have reduced band gaps relative to their II-VI analogs as a result of the presence of the  $d$  levels. Robbins<sup>3</sup> also attributes discrepancies in the tetragonal distortion model of Abrahams and Bernstein<sup>4</sup> to the  $d$  levels. From electroreflectance measurements of the spin-orbit splitting at the top of the valence band, a  $p$ - $d$  hybridization of (16–45)% in the I-III- $V_2$  valence bands is reported.<sup>1</sup>

Since the chalcopyrite primitive cell contains eight atoms, the Brillouin zone has one-fourth the zinc-blende zone volume and the chalcopyrite zone can be obtained by folding-in the zinc-blende zone

with reciprocal-lattice vectors  $\Gamma$ ,  $W_x$  ( $2\pi/a, 0, \pi/a$ ),  $W_y$  ( $0, 2\pi/a, \pi/a$ ), and  $X_z$  ( $0, 0, 2\pi/a$ ).<sup>1, 6-9</sup> The folding-in also leads to a number of "pseudodirect" energy gaps<sup>1, 8</sup> which have a significance to be discussed below.

Band structures have been calculated by the empirical pseudopotential method at the high-symmetry points ( $\Gamma, X, A, Z$ ) for  $\text{ZnGeP}_2$ ,<sup>10</sup>  $\text{ZnGeAs}_2$ ,<sup>10</sup>  $\text{AgInSe}_2$ ,<sup>11</sup>  $\text{CuInSe}_2$ ,<sup>12</sup> and  $\text{CuGaS}_2$ ,<sup>12</sup> and at many points in the zone for  $\text{ZnGeP}_2$  by de Alvarez *et al.*<sup>8, 13</sup> Because the I-III-VL<sub>2</sub> pseudopotential calculations do not explicitly include the effects of  $d$  levels in the conduction band they are difficult to relate to experiment and will not be referred to in what follows.

### III. PROCEDURES

The synchrotron source, monochromator, reflectivity chamber, and computer acquisition of data have all been recently described<sup>14, 15</sup> with general references to vacuum-ultraviolet studies and techniques. Our specimens, some in bulk polycrystalline form and others in the form of single crystals with (112) growth-plane faces, were all prepared at the Bell Laboratories. The (112) face is equivalent to the (111) face in zincblende crystals and the  $\vec{E} \parallel \vec{c}$  polarization for such crystals is only nominal since the  $c$ -axis projection on the (112) face is about 65%. Because the chalcopyrites are very difficult to cleave and because the bulk samples were polycrystalline in many cases the bulk samples were cut and polished for the reflectivity measurements. Of course, the true crystal reflectivity spectra will be dulled depending on the extent of surface layer damage due to polishing. The final polishing procedure for all specimens was developed from experience and consisted of a "Syton"<sup>16</sup> polish and etch and then an etch in concentrated  $\text{NH}_4\text{OH}$  [(20-30)%  $\text{NH}_3$ ] at room temperature for 30 sec. Reflectivity structure was generally not as high or sharp without the final polish and etch but no new features were introduced. Once in place, the specimen could be rotated to change the angle of photon incidence. For all reflectivity data reported here, the angle of incidence was about 12°. The specimen could also be raised or lowered for measurement of the incident and reflected intensities with a sodium-salicylate-coated rotatable lightpipe, rotated around the surface normal to obtain various orientations with respect to the incoming light polarization, and cooled to 30 K with liquid helium. The reflectivity data reported in this paper are all at 80 K since lower temperatures yielded little additional sharpening. Although the I-III-VL<sub>2</sub> and particularly the silver chalcopyrites have an unusual band-gap temperature depen-

dence,<sup>17, 18</sup> we observed only typical phonon-density-dependent shifts of reflectivity features above the band gap. Our XPS spectra were obtained at room temperature. Relative energy shifts between 80 and 300 K are small, much less than XPS resolution ( $\sim 0.55$  eV) and will be ignored.

In the reflectance experiments, light intensities were measured with photo-multipliers and photon-counting techniques. Real-time adjustments were made for constant statistics (if desired), for normalization of beam current in the electron storage ring, for incident intensity, and for dead time corrections. Data for  $E < 8$  eV were taken with a quartz filter to reduce the second-order monochromator light intensity; a  $\text{MgF}_2$  filter was used from 5 to 11 eV. No filter was used in scans from 8 eV to the highest energies. For photon energies below 2.4 eV our data were unreliable because of properties of the sodium-salicylate-coated lightpipe. A more serious experimental problem arose in the 10-12 eV range resulting from the use of a  $\text{MgF}_2$ -overcoated aluminum grating. An artifact arose which our measurement procedures could not eliminate. The artifact, which took the form of an apparent dip in reflectivity near 11 eV, could be eliminated with the use of a gold grating. This grating, however, was not useful for much of the energy range of interest. Thus we have corrected our data in the 10-12 eV range to minimize the influence of the artifact. In general, absolute reflectivity errors of (2-3)% could have arisen through surface and crystalline defects but only near 11 eV was any difference in reflectivity structure found under differing conditions. Optical constants were calculated<sup>19</sup> by a Kramers-Kronig inversion<sup>20</sup> of the reflectivity data including a match to infrared data<sup>1, 21</sup> but will not be presented here.

We have used XPS measurements along with calculated atomic core level energies<sup>38</sup> to determine the core level and valence-band contributions to the reflectivity. A description of this procedure is given elsewhere.<sup>5, 22</sup> The XPS data were taken with a Hewlett-Packard 5950A spectrometer employing monochromatized aluminum  $K\alpha$  radiation. The resolution is  $\sim 0.55$  eV. Data were taken on samples that were cleaved (crushed) immediately prior to insertion into the spectrometer. Because only very weak 1s lines of oxygen and carbon were observed, effects of surface contamination are believed to be minimal.

### IV. RESULTS AND DISCUSSION

#### A. $\text{CuGaS}_2$

Two specimens were studied, namely, stoichiometric  $\text{CuGaS}_2$  and  $\text{Cu}_{0.88}\text{Ga}_{1.04}\text{S}_2$ . Both were single crystals with (112) growth faces. Figure 1

shows the reflectivity of  $\text{CuGaS}_2$  at 80 K for each polarization. The reflectivity of  $\text{Cu}_{0.88}\text{Ga}_{1.04}\text{S}_2$  is very similar. The  $\vec{E} \parallel \vec{c}$  polarization is only nominal since the growth face was the reflecting plane. Orientation is easily done *in situ* since the anisotropy of the exciton peaks is very pronounced.<sup>1, 24</sup> Unpolarized reflectivity measurements have previously been made on  $\text{CuGaS}_2$  to 11 eV,<sup>25</sup> and on an orange, nonstoichiometric specimen to 5.6 eV,<sup>26</sup> but additional structure is evident in our measurements for the same energy ranges. Reflectance features associated with transitions from the Ga 3d core levels (Ga-3d "core reflectivities") are shown in blowup near 22 eV in Fig. 1. Transitions from the 3d core states enable us to identify portions of the conduction band that have flat *p*-like character. The combination of reflectivity and XPS spectra, shown in Fig. 2, permits some general statements to be made about the band structure. An XPS spectrum was previously reported but only to 9 eV below the top of the valence band.<sup>27</sup> Using x-ray and uv photoemission spectra, the separation of *p*- and *d*-like regions of the valence-band structure has been made for the related compound  $\text{CuInS}_2$ .<sup>23</sup> From those results, we infer that the overlying  $\text{CuGaS}_2$  XPS peak 2 eV below the top of the valence band ( $V_0$  in Fig. 2) derives mostly from the Cu 3d states with some S-3*p* admixture. At higher energies in Fig. 2  $V_4$  is, by analogy with  $\text{ZnGeP}_2$ ,<sup>39</sup> probably a peaking of the *s*-electron density of states around the cations while  $V_5$  is the S 3s states. The Ga-3d spin-orbit doublet appears near -19 eV. Reflectivity features for  $\text{CuGaS}_2$ , as for all the specimens studied, are tabulated in Table I and identified XPS features are listed in Table II. In principle, energy spacings of levels observed in XPS and optical absorption need not coincide because of energy shifts which result from excitonic

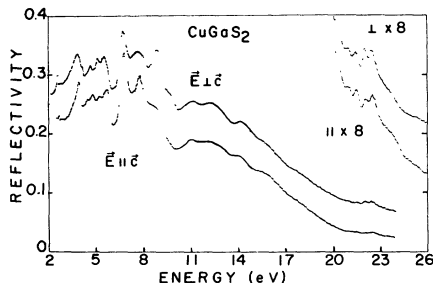


FIG. 1. Reflectivity of  $\text{CuGaS}_2$  from 2 to 26 eV. For  $\vec{E} \perp \vec{c}$  the reflectivity is shifted upwards by 0.05 relative to its absolute location for clarity. The reflectivity near 22 eV is also multiplied by a factor of 8 and shifted arbitrarily. Data are computer output plots except near 11 eV where an artifact was removed by hand as discussed in the text. Specimen temperature was 80 K.

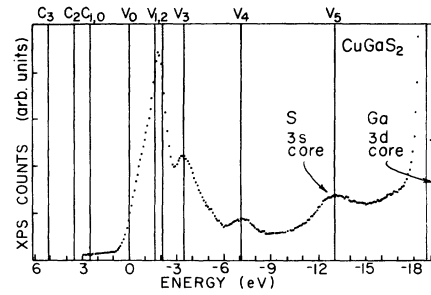


FIG. 2. XPS data for  $\text{CuGaS}_2$  with identified critical levels in conduction and valence bands. The Ga 3d core levels are roughly 19 eV below the top of the valence band  $V_0$ . The state  $V_5$  is attributed to sulfur 3s core states.  $V_4$  probably identifies *s* states centered on the cations and  $V_1$  and  $V_2$  are predominately Cu 3d in character (see text).

or final-state interactions.<sup>28</sup> Generally we will assume that energy shifts are small, of order 0.2 eV or less as has been suggested for GaP and GaAs.<sup>5, 29</sup> However, for  $\text{CuGaS}_2$  it appears that the XPS measurement of the separation of the valence band edge  $V_0$ , and the Ga-3d core is at least 0.3 eV larger than the same separation inferred from reflectivity measurements (19.0 vs 18.7 eV, respectively). Furthermore, this minimum energy shift applies only if the lowest final state ( $C_1$ ) of the 3d to conduction-band transition is close to the bottom of the conduction band at the center of the zone. (The conduction-band minimum is always called  $C_0$  in this paper.) In no case for our I-III-VI<sub>2</sub> chalcocopyrites do we actually find that the lowest final state of a "core reflectivity" can be distinguished from the state  $C_0$  which is a band-gap energy above  $V_0$ . In several of the succeeding figures, the two states,  $C_0$  and  $C_1$ , show the maximum energy difference which is consistent with our observation if there are indeed two conduction-band states.

The Ga 3d core states are initial states for two sharp pairs and two broader transitions and appear to define four conduction states labeled  $C_1$ - $C_4$ . The energies of these states relative to  $V_0$  are indicated in Table II along with the energies of particular valence band or core features. The two spin-orbit ( $d_{5/2}$  and  $d_{3/2}$ ) components of both sharp transitions are resolved in reflectivity with the expected<sup>29</sup> 0.45 eV splitting; for the broad transitions the components are not resolved. Gudat *et al.* observed equivalent but less well resolved Ga-*d* "core reflectivity and absorption" in samples of GaAs, GaP, and GaSb.<sup>5</sup> Their data indicated that reflectivity structure due to transitions from the almost flat Ga 3d levels maps out the conduction-band density of states. More recently GaAs and GaP electroreflectance measurements of Aspnes, Olson, and

TABLE I. Energies (in eV) of prominent reflectivity features at 80°K.

CuGaS <sub>2</sub>		CuAlS <sub>2</sub>		CuInSe <sub>2</sub>	AgInSe <sub>2</sub>	ZnGeP <sub>2</sub>		ZnGeAs <sub>2</sub>
Nominal $\bar{E} \parallel \bar{c}$	$\bar{E} \perp \bar{c}$	Nominal $\bar{E} \parallel \bar{c}$	$\bar{E} \perp \bar{c}$			$\bar{E} \parallel \bar{c}$	$\bar{E} \perp \bar{c}$	
2.48	...	3.50	...	2.90	3.28	3.04	3.02	2.46
...	2.60	3.62	3.62	3.68	3.50	3.20	3.25	2.70
2.62	...	4.33	4.33	4.85	4.18	3.44	3.42	3.24
3.84	3.82	4.84	4.96	5.38	5.0	3.68	3.72	3.46
...	4.20	5.46	5.44	6.18	5.9	4.18	4.20	3.8
4.40	...	5.70	5.70	6.70	6.8	4.44	{ 4.38 ?	4.50
4.70	4.68	7.0	7.0	7.60	7.20		{ 4.46 ?	4.92 ?
5.14	5.12	7.82	7.91	9.30	8.9		{ 4.75 ?	
5.58	5.56	9.0	9.0	11.1	11.2	4.86	{ 4.86	5.06
6.70	6.70	11.2	11.2	12.0 ?	12.6 ?	5.2	5.2	5.36
7.7	7.7	12.4	12.4	13.6	13.0 ?	5.6	5.6	5.70
8.9	8.9	14.2	14.2	18.55	14.5 ?	6.2	6.2	6.0
...	9.7	16.1 } 16.6 }	16.3	19.5	17.6	6.6	6.6	6.7
11.0	11.0			20.0 ?	18.5	7.1	7.1	7.6
12.5	12.5			20.8	19.4	7.9	7.9	8.0
14.1	14.2				20.2	9.6	9.6	9.6
15.7	15.7				20.9	11.7	11.7	11.7
18.0	18.0				21.8	13.1	13.1	13.0
21.025	21.025					14.2	14.2	14.2
21.475	21.475					16.0	16.0	16.0
22.05	22.05							
22.50	22.50							
23.75	23.75							
25.50	25.50							

Lynch<sup>29</sup> indicate however, that in line with atomic selection rules transitions to final states  $p$  like around the Ga cation, such as at  $X_1$ , are most probable. Indeed, atomic selection rules appear to describe the relative intensities and polarization dependences of the Ga-3d sharp transitions in CuGaS<sub>2</sub> (as for the "core reflectivities" in the lead salts<sup>22</sup>), but this may be fortuitous.<sup>19</sup> The final states  $C_3$  and  $C_4$ , although  $p$ -like, may contain considerable curvature since the spin-orbit splitting is unresolved. Unfortunately the data does not locate any transitions in the zone. The  $p$ -like regions in the conduction band also appear to act as final states for other transitions from the valence bands observed at lower energies. But the dominating effects of  $E_1$ - and  $E_2$ -like transitions, common in many other semiconductors,<sup>30</sup> are suspected in all of our specimens. However, a different interpretation has been advanced for the major low-energy peak in CuInSe<sub>2</sub>.<sup>31</sup> In alloy studies on the CuInSe<sub>2</sub>-ZnSe system,<sup>31, 32</sup> Gan *et al.* observed a sudden appearance or shift of the major low-energy structure in the alloy at the phase change to the chalcopyrite structure and concluded that a new pseudo-direct transition from  $V_0$  to a folded-in-zinc-blende state of  $X$  symmetry was responsible. Whereas the joint density of states for this pseudo-direct transition might be favorable, theoretical

calculations of the matrix element<sup>8</sup> predict such  $\bar{k} - \bar{k} + \bar{X}_z$  transitions to be weak in the II-IV- $V_2$  chalcopyrites; and indeed they have been observed so in ZnGeP<sub>2</sub>.<sup>8, 39, 41</sup> The possibility of large structure in the I-III-VI<sub>2</sub> chalcopyrite reflectivity appears to rest on a strong alteration of the transi-

TABLE II. Energy location (in eV) of identified XPS and density-of-states regions relative to the indicated top of the valence band (see Figs. 2, 5, 7, 9, and 11). Correlation of labels not necessarily implied between specimens for levels  $C_1$ ,  $C_2$ ,  $C_3$ ,  $C_4$ ,  $V_1$ ,  $V_2$ , and  $V_3$ .

Level	CuGaS <sub>2</sub>	CuInSe <sub>2</sub>	AgInSe <sub>2</sub>	ZnGeP <sub>2</sub>	ZnGeAs <sub>2</sub>
$C_4$	6.8	...	...	4.6	4.8
$C_3$	5.1	3.4	4.5	3.5	3.7
$C_2$	3.5	2.9	3.0	2.1	2.5
$C_1$	2.5	1.4	1.3	...	...
$C_0$	2.5	1.1	1.3	2.4	1.2
$V_0$	0.0	0.0	0.0	0.0	0.0
$V_1$	-1.6	-2.1	-1.0	-0.9	-0.3
$V_2$	-2.1	-2.1	-4.3	...	-0.9
$V_3$	-3.4	-3.3	-4.3	-3.0	-2.9
$V_4$	-7.1	-6.3	...	-7.3	-7.1
$V_5$	-13.0	-13.0	-12.4	-12.8	-13.0
Core					
$d_{5/2}$	-18.8	-17.2	-16.7	-9.3	-9.2
$d_{3/2}$	-19.3	-18.0	-17.6	-9.8	-9.7

tion probability due to the presence of  $d$  levels in the valence band. We will consider other interpretations as well.

Tell and Bridenbaugh<sup>33</sup> have shown for  $\text{CuGaS}_2$  that the uppermost valence band has mixed  $d$  and  $p$  character. That band arises from the Cu  $d$  levels hybridized with sulfur  $p$ -like states of the same,  $\Gamma_{15}$ , symmetry. The valence band is expected to be shifted up by about 1.4 eV relative to the II-VI analog, thus lowering the energy gap. Noninteracting  $d$  levels of Cu, with  $\Gamma_{12}$  symmetry at the center of the zone, should be found roughly 1.2 eV below the top of the valence band. Another  $p$  and  $d$  admixed spin-orbit doublet is expected to be about 2 eV below the top of the valence band at the zone center. This description is not inconsistent with our XPS spectrum which shows a strong peak (labeled  $V_1$  and  $V_2$  in Fig. 2) at 2 eV below  $V_0$ . The  $V_1$  and  $V_2$  labels are derived from the reflectivity spectrum as follows. Four small and sharp reflectivity peaks are observed between 4.15 and 5.7 eV for both polarizations, but at slightly higher energies for  $\vec{E} \parallel \vec{c}$ . The transitions appear to be in two pairs (on the  $\vec{E} \parallel \vec{c}$  spectrum) roughly 0.5 eV apart. These small peaks appear to be superposed on a large reflectivity structure (at 5.6 eV) the steep edge of which is at 5.8 eV. In an interpretation consistent with the general model of Tell and Bridenbaugh,<sup>33</sup> the small and sharp structures arise from transitions near the zone center to the vicinity of the conduction-band states previously identified from the Ga- $3d$  core reflectivity. The four sharp peaks could also represent transitions from unhybridized Cu  $3d$  states to the  $p$ -like conduction band states (but not necessarily at  $\Gamma$ ).  $V_1$  and  $V_2$  would then denote the Cu  $3d$  spin-orbit doublet. The peak at 3.8 eV, in analogy with the interpretation advanced by Gan *et al.*<sup>31</sup> for  $\text{CuInSe}_2$ , could be a pseudodirect transition from  $V_0$  to a state about 0.2 eV above  $C_2$  and at the center of the zone. However, we find no other evidence for such a final state. In all our specimens it is possible to make a more conventional assumption that the lowest dominant transition (3.8 eV in  $\text{CuGaS}_2$ ) is an analog of the  $E_1$  transition which occurs in many other semiconductors.<sup>30, 34</sup> The reflectivity feature may result from a Van Hove singularity which occurs away from the zone center in near but accidental degeneracy with  $V_0$ - $C_2$ . In fact, the four strong transitions at 3.8, 5.6, 6.7, and 8.9 eV may be associated with pairs of  $E_1$  and  $E_2$  transitions from the upper and lower  $p$ - $d$  hybridized bands of Tell and Bridenbaugh<sup>33</sup> away from the zone center. In correspondence with the ZnS analog,<sup>34</sup> we suggest that the 3.8 and 6.7 eV peaks result from  $E_1$  transitions. (An alternate possibility is that  $E_1$  transitions account for the 3.8 and 5.6 eV peaks.) The highly anisotropic

nature of the 7.7 and 8.9 eV peaks should be particularly significant. The 8.9 eV peak ( $\vec{E} \perp \vec{c}$ ) appears to result from a transition which is forbidden for  $\vec{E} \parallel \vec{c}$  and occurs near the predicted  $V_3$  to  $C_3$  energy difference. However, a full band calculation is needed to reduce the ambiguity in this assignment.

Other interpretations could be presented for the peaks from 6.7 through 9 eV, particularly since weaker structure, in addition to the major features, is also visible. Specifically, the 6.7 eV peak, which is stronger for  $\vec{E} \parallel \vec{c}$  than for  $\vec{E} \perp \vec{c}$ , is found to be a doublet at room temperature for  $\vec{E} \perp \vec{c}$ . The 8.9 eV peak for  $\vec{E} \parallel \vec{c}$ , when studied under high resolution and precision at 80 K, is also found to be a doublet. The 6.7 eV peak, which appears near the energy separations  $V_1$ - $C_3$  and  $V_3$ - $C_2$ , also gives rise to a very strong temperature-modulation signal. One final observation may eventually be useful. In  $\text{Cu}_{0.88}\text{Ga}_{1.04}\text{S}_2$  the major difference in reflectivity from that of the stoichiometric specimen occurs for the 6.7 to 8.9 eV peaks which are both considerably weaker than their counterparts in the stoichiometric specimen.

Extending the atomiclike transition analysis the energy location of the four peaks observed between 10.5 and 14 eV suggests  $s$ - $p$  transitions from initial states  $V_4$ ,  $s$ -like around the cations, to the  $C_1$ - $C_4$  final states while the broad, poorly resolved, transitions centered at 15.7 and 18.0 eV could originate at  $V_5$ , the sulfur  $3s$  core band, and terminate in the  $C_{1,0}$  and  $C_3$  regions, respectively.

## B. $\text{CuAlS}_2$

We now consider the changes in reflectivity which take place when aluminum replaces gallium in the chalcopyrite  $\text{CuGaS}_2$ . The interpretation becomes less certain because a number of reflectivity features associated with the gallium  $3d$  levels are no longer present. Our specimen was a small crystal with a (112) growth face, too small for convenient XPS measurement, but such measurements have been reported<sup>27, 35</sup> up to 10 eV below the top of the valence band with results similar to those found in  $\text{CuGaS}_2$ . Figure 3 shows our measured reflectivities at 80 K for both polarizations. A few general remarks can be made. The exchange of aluminum for gallium seems to have two major effects. First, the band gap increases to 3.49 from 2.43 eV (Ref. 1) and the large interband peak at 4.8 eV (probably an  $E_1$  structure or absorption associated with folded-in  $X_z$  states by analogy with  $\text{CuInSe}_2$ )<sup>31</sup> now appears to overlap weaker peaks associated with transitions from valence states comparable to the  $\text{CuGaS}_2$  states  $V_1$  and  $V_2$  in Fig. 2. The sharp structure seen at 4.33 eV would be  $V_1$ - $C_{1,0}$  in this

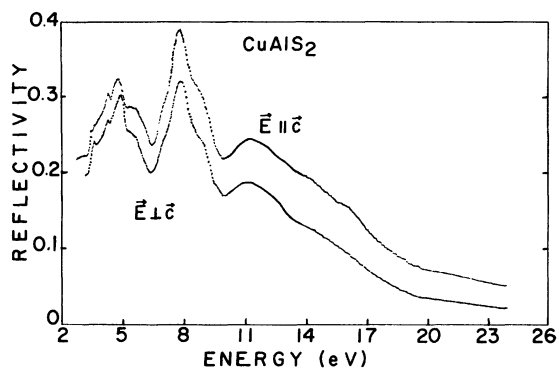


FIG. 3. Reflectivity of  $\text{CuAlS}_2$  at 80 K from 2 to 26 eV. For clarity, the  $\vec{E} \parallel \vec{c}$  polarization is shifted upwards by 0.025 relative to its absolute location. Data are computer-file output plots except near 11 eV where an artifact was removed by hand as discussed in the text.

interpretation thus locating  $V_1$  at 0.86 below  $V_0$ . Second, the three large peaks from 6 to 9.5 eV in  $\text{CuGaS}_2$  have apparently merged to a considerable extent in  $\text{CuAlS}_2$  and major anisotropies are no longer evident. The features between 10 and 20 eV are similar and probably have a common description.

### C. $\text{CuInSe}_2$

Our specimen was cut from the bulk, polished, and left unoriented. Since the crystalline field is almost zero ( $2 - c/a \approx 0$ ) the orientation was not expected to affect the larger structures observed in reflectivity although transitions from the copper  $d$  levels have been observed in electroreflectance to be anisotropic as a result of tetragonal distortion.<sup>1, 17, 36</sup> Figure 4 shows the reflectivity at 80 K and Fig. 5 the XPS spectrum for our specimen. From the  $\text{CuInS}_2$  x-ray and uv photoemission results<sup>23</sup> we infer that the shoulder at  $-0.5$  eV and the overlying peak at  $-2.1$  eV in our XPS data on  $\text{CuInSe}_2$  derive mostly from the Cu  $3d$  states. Like  $\text{CuGaS}_2$ , the  $d$  states probably contain a substantial

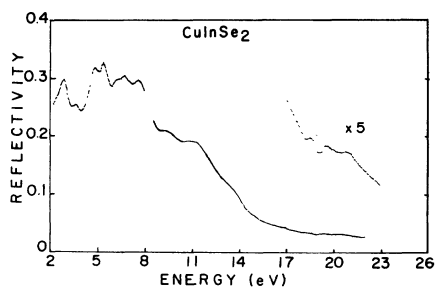


FIG. 4. Reflectivity of unoriented  $\text{CuInSe}_2$  at 80 K. Near 20 eV, the reflectivity is also multiplied by a factor of 5 and shifted arbitrarily. Data are computer-file output plots except near 11 eV where an artifact was removed by hand as discussed in the text.

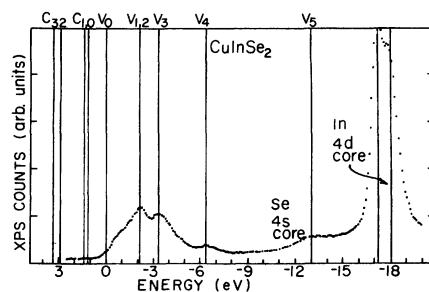


FIG. 5. XPS data for  $\text{CuInSe}_2$  with identified or inferred critical levels in conduction and valence bands. The In  $4d$  core levels are roughly 17.6 eV below the top of the valence band  $V_0$ . The state  $V_5$  is attributed to Se  $4s$  core states.  $V_4$  probably identifies  $s$  states centered on the cations and states  $V_{1,2}$  are predominately hybridized Cu  $3d$  states (see text).

$p$ -state admixture. The  $-2.1$  eV peak is significantly suppressed relative to the similar structure shown in Fig. 2 for  $\text{CuGaS}_2$ . The lowest valence-band peak at  $-6.3$  eV may be related to the light hole band of the analog substance  $\text{Zn}_{0.5}\text{Cd}_{0.5}\text{Se}$  or to states which are  $s$ -like around the cations.<sup>39</sup> The Se  $4s$  and In  $4d$  core levels appear at  $-13$  and  $-17.6$  eV, respectively. The spin-orbit splitting of the In  $4d$  levels in  $\text{CuInS}_2$  is 0.80 eV,<sup>23</sup> consistent with the barely resolved doublet seen in our XPS spectrum. We use a calculated value<sup>38</sup> of 0.86 eV for our analysis.

Electroreflectance measurements for  $\text{CuInSe}_2$  have been reported<sup>17, 36</sup> and Gan *et al.*<sup>31, 32</sup> have measured the reflectivities of  $(\text{CuInSe}_2)_{1-x}(\text{ZnSe})_x$  from 0.5 to 14 eV for eight samples with different values of  $x$  and have analyzed their results on the basis of a ZnSe band structure folded into the chalcopyrite zone. Our  $\text{CuInSe}_2$  reflectivity compares reasonably well with theirs except that we find additional structure at 3.68, 6.2, and 9.3 eV and the magnitudes of our peaks at 4.85 and 5.38 eV are relatively higher. Above 14 eV we report new In- $4d$  "core reflecting" structure similar to that seen by Gudat *et al.* in InAs, InP, and InSb.<sup>5</sup> In accord with the interpretation for  $\text{AgInSe}_2$  below the In  $4d$  core states are used to locate three conduction-band regions, designated  $C_1$ ,  $C_2$ , and  $C_3$  in Fig. 5.  $V_0$  is placed at the valence-band edge with  $C_0$  a band-gap energy above at 1.1 eV. Unlike  $\text{CuGaS}_2$ , it is not necessary to assume a relative shift between energy levels obtained from XPS and reflectivity data since  $C_1$  appears at a higher energy than  $C_0$ . However, a shift of up to 0.3 eV is also consistent with the general interpretation.

In the alloy measurements of Gan *et al.*,<sup>32</sup> the 2.90 eV peak apparently appears at the zinc blende-to-chalcopyrite phase change and persists in the

chalcopyrite structure. The 4.85 eV peak is thought to persist as an  $E_1$  structure for the entire alloy range. The interpretation was advanced that the 2.90 eV peak results from a pseudodirect transition. Another possibility is that the  $E_1$  structure makes an abrupt transition to lower energy (in the chalcopyrite phase) at the transition from zincblende-to-chalcopyrite structure. Using the Tell and Bridenbaugh<sup>33</sup> model for  $\text{CuGaS}_2$  as a guide, we can attribute the 2.90 eV peak in  $\text{CuInSe}_2$  to an  $E_1$ -like transition from the upper  $p$ - $d$  hybridized band. The small 3.68 eV peak in reflectivity is associated with transitions from the noninteracting copper  $d$  levels. As for  $\text{CuGaS}_2$ , the 2.90 eV peak is in near coincidence with the separation energy  $V_0$ - $C_2$  and probably overlaps transitions from  $V_{1,2}$  to the lower conduction bands as in  $\text{CuGaS}_2$  and  $\text{AgInSe}_2$ . The very complicated electroreflectance spectrum in this energy range<sup>17,36</sup> may be noted. A number of possible explanations could be advanced to interpret the reflectivity structure between 4.8 and 6.7 eV in terms of  $E_1$  and  $E_2$  transitions from both upper and lower  $p$ - $d$  hybridized bands. However, none of these choices could be clearly justified. The 7.60 and 9.3 eV reflectivity structures agree well with energy spacings between  $V_4$  (assumed to be associated with states  $s$ -like around cations) and the  $p$ -like final states  $C_1$  and  $C_2$ . From the alloy data,<sup>32</sup> it appears that the reflectivity rise near 11 eV is associated with an  $E'_1$  transition. The weak shoulder at 13.6 eV can probably be attributed to transitions from the 3s core level of selenium,  $V_5$ , although the indicated energy of  $V_5$  appears to be about 0.5 eV too low.

#### D. $\text{AgInSe}_2$

The specimen was a polycrystalline bulk sample with a polished surface that was covered with tiny cracks. The relatively low magnitude of the reflectivity

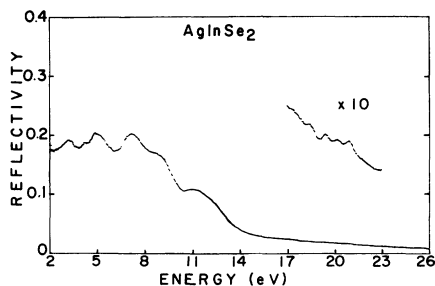


FIG. 6. Reflectivity of  $\text{AgInSe}_2$  at 80 K. Specimen was polycrystalline with poor surface quality. The reflectivity near 19 eV also appears multiplied by a factor of 10 and arbitrary offset. Six peaks could be identified in three pairs with 0.86 eV spacing, the expected spin-orbit splitting of  $\text{In } 4d$  states.

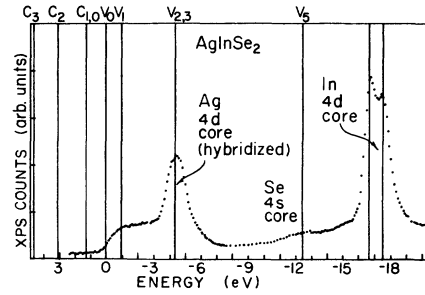


FIG. 7. XPS data for  $\text{AgInSe}_2$  with valence and conduction levels indicated as discussed in the text. The  $\text{Ag-}4d$  spin-orbit splitting is not resolved but the splitting is seen for the  $\text{In } 4d$  core states. Hybridization of the  $\text{Ag-}4d$  core is shown in Ref. 1 to be small.

ity (80 K data are shown in Fig. 6) probably results from the poor optical quality of the reflecting surface. Little sharpening of the reflectivity peaks was observed at 80 K relative to measurements at room temperature. The XPS spectrum, displayed in Fig. 7, is similar in appearance to that of  $\text{CuInSe}_2$  except that the silver  $d$  levels lie deeper in the valence band than do those of copper. The silver  $d$  states hybridize less with selenium  $p$  states at the top of the valence band than do the copper  $d$ -states in  $\text{CuInSe}_2$  (17% vs 34% from electroreflectance measurements<sup>1</sup>). Thus the  $\text{AgInSe}_2$   $d$  bands are flatter and the band-gap shift from the II-VI analog is less than for the case of  $\text{CuInSe}_2$ . The XPS spectrum shows the  $\text{In } 4d$  spin-orbit-split core levels to be resolved, but the spin-orbit components of the  $\text{Ag } 4d$  states (for which a splitting of 0.65 eV is expected<sup>38</sup> are not resolved. Reflectivity features associated with the indium core levels contain six resolved peaks in three pairs. These features define three flat  $p$ -like regions in the conduction band which are designated  $C_1$ ,  $C_2$ , and  $C_3$  in Fig. 7. Core levels determined from reflectivity data are apparently shifted about 0.4 eV to lower energies than the XPS level energies.

Comparison of the gross features of the reflectivity of  $\text{AgInSe}_2$  with its analog  $\text{CdSe}$  [wurtzite structure at 100 K (Ref. 34)] and with  $\text{CuInSe}_2$  reveals several similarities. The  $\text{CdSe } E_1$  peak at 4.95 eV and the  $E_2$  feature at 7.6 eV might appear closely related to the 5.0 and 7.20 eV major peaks in  $\text{AgInSe}_2$  and the small impact of hybridization in the latter could justify such a correspondence. The 3.3 eV peak, like the 2.9 peak in  $\text{CuInSe}_2$ , might then be described by the model of Gan *et al.*<sup>32</sup> as a transition to the band folded-in by  $X_z$  in the band structure calculated for  $\text{AgInSe}_2$ .<sup>11</sup> As with other spectra reported in this paper, the first major peak (3.3 eV in  $\text{AgInSe}_2$ ) appears close in energy to the separation  $V_0$ - $C_2$ . However since  $p$ - $d$  hybrid-

ization is minimal in  $\text{AgInSe}_2$  it seems unlikely that pseudodirect transitions are responsible for dominant reflectivity features such as the 3.3 eV peak. It is also possible to describe the 3.3 eV peak as in  $E_1$  reflectivity feature and the higher-energy features in terms of other  $E_1$  and  $E_2$  transitions. The energy difference between the band gap and  $E_1$  peak in  $\text{CdSe}$  (Ref. 34) is roughly maintained in  $\text{AgInSe}_2$  if the 3.3 eV peak is an  $E_1$  transition.

The Ag  $4d$  core states do not appear to produce sharp reflectivity features but both strong and also weak and poorly resolved features appear at energies corresponding to  $V_{2,3}-C_{1,2,3}$ . Energy separations between the initial states identified from XPS measurements and the flat  $p$ -like final state regions identified from the "core reflectivities" are suggestively close to reflectivity structure observed at lower energies and may indicate some bunching of conduction-band states near the flat  $p$ -like regions. A valence-band critical energy,  $V_1$ , has been inserted 1.0 eV below  $V_0$  to account for two important reflectivity features. Although the band gap of  $\text{AgInSe}_2$  displays no shift from liquid nitrogen to room temperatures ( $0 \pm 5$  meV)<sup>11, 17</sup> the peaks at 3.3, 4.18 and 5.0 eV were all about  $0.075 \pm 0.020$  eV lower in energy at room temperature than at 80 K.

### E. $\text{ZnGeP}_2$

Our sample was cut from the bulk, polished, and oriented with the  $c$ -axis in the specimen plane. Figure 8 shows the reflectivity at 80 K for the  $c$ -axis perpendicular and parallel to the polarization of the radiation. Structure in the region of the band gap for  $E < 5$  eV has been well studied by thermoreflectance<sup>40</sup> and electroreflectance<sup>41</sup> techniques. Our data are in good accord with earlier reflectivity measurements at 5 K in the region below 5 eV.<sup>8</sup>

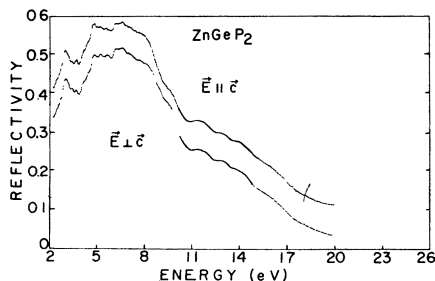


FIG. 8. Reflectivity of  $\text{ZnGeP}_2$  at 80 K for two polarizations from 2 to 20 eV. Data are computer output plots except near 11 eV where corrections were made by hand as discussed in the text. The reflectivity for  $\vec{E} \parallel \vec{c}$  is shifted vertically by 0.075 for clarity. Many small reflectivity features were observed and are tabulated in Table I.

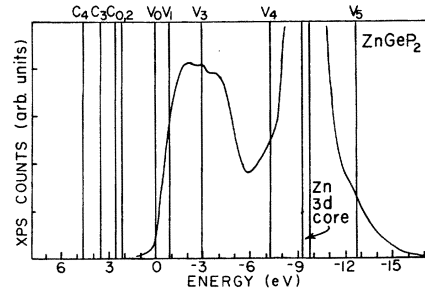


FIG. 9. XPS data for  $\text{SnGeP}_2$  according to de Alvarez *et al.* (Ref. 39). Valence and conduction-band levels are indicated as discussed in the text. The inverted ordering at the bottom of the conduction band was suggested by the evidence for pseudo-direct energy gap features as discussed in Ref. 1.

De Alvarez *et al.*<sup>8</sup> interpret their data with reference to an accompanying band calculation. (In fact,  $\text{ZnGeP}_2$  may be the best characterized ternary chalcopyrite because detailed electronic-band-structure calculations have been made<sup>8, 13, 37</sup>). Although the calculation<sup>8</sup> does not reproduce the pseudo-direct ordering at the bottom of the conduction band, it does designate many critical points in the zone. In brief, their interpretation is the following. The first peak at 3.0 eV and the rise at 4.0 eV are derived from the  $E_1$  and  $E_2$  features in GaP, respectively. The bump at 4.8 eV is assigned to transitions near  $X_1$  (involving bands 16 to 20 in Fig. 4 of Ref. 8, where the valence bands are numbered 1 to 16 and the conduction bands from 17 on). Our reflectivity data reveal a triplet of bumps at 4.8, 5.2, and 5.6 eV which we attribute to  $X$  and related  $N$  plane transitions (bands 16–20, 14–20, and 12–20 of Ref. 8) arising from the  $L_3$  and  $\Sigma_1$  levels in GaP which are calculated to be close in energy for the  $B^N C^{8-N}$  semiconductors.<sup>8, 42</sup>

The two peaks at 6.2 and 6.6 eV could correspond to the  $E'_1$  and  $E'_1 + \Delta'_1$  peaks in GaP as has been suggested for  $\text{CdGeP}_2$ ,<sup>43</sup> and likely transitions would be in the  $N$  plane in the directions  $N(x, x, 2x)$  and at  $A_1-A_2$  (bands 10–20 of Ref. 8). The origin of string reflectance near 8 eV is unknown. The broad shoulder at 9.6 eV could be related to the  $E''_1$  transition observed in the electroreflectance spectrum of GaP at 10.7 eV.<sup>29</sup> XPS data and band-structure calculations<sup>39</sup> show an appreciable density of  $s$ -like states around the cations at energies 6–8 eV below the top of the valence band as shown in Fig. 9 (reproduced from Ref. 39). Transitions from these states to  $p$ -like states in the conduction band probably contribute to the broad 9.6-eV feature. Absorption above 11 eV results in part from transitions originating at the Zn  $3d$  and P  $3s$  states and terminating at  $p$ -like conduction band states. Transitions from the upper valence bands may also



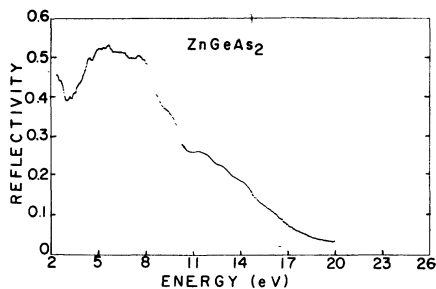


FIG. 10. Reflectivity of  $\text{ZnGeAs}_2$  at 80 K from 2.5 to 20 eV. The three broad reflectivity features from 11.5 to 14 eV are similar to those we found in  $\text{ZnGeP}_2$  and are probably associated with Zn  $3d$  core states. Their energies are used to locate the conduction band states labeled in Fig. 12. The broad peak at 16 eV apparently has an As  $4s$  initial state. The strong similarity to the gross features of the  $\text{ZnGeP}_2$  reflectivity (Fig. 9) is evident.

contribute. Although the Zn  $3d$  spin-orbit splitting is not resolved with XPS, it seems likely that the 11.7, 13.0 and perhaps the 14.2 eV bumps in the reflectivity are associated with the Zn  $3d$  levels just as similar structure has been attributed to the Cd  $d$  levels in CdTe by Gudat *et al.*<sup>5</sup> The deduced final conduction-band state  $C_2$  (Fig. 9) appears 0.3 eV below the direct gap edge,  $C_0$ , in agreement with the experimental pseudodirect gap<sup>8, 40, 41</sup> and the expectation that the  $\Gamma$ -mapped, zinc-blende-analog  $X_1$  state is  $p$ -like around the cation.<sup>29</sup> The 14.2 eV and more probably the 16.0 eV peaks could originate from the upper (2-4) and lower (1) P-3s bands.

#### F. $\text{ZnGeAs}_2$

Our  $\text{ZnGeAs}_2$  specimen was a polished polycrystalline bulk sample. Figure 10 shows the reflectivity at 80 K and Fig. 11 shows the XPS spectrum. Electroreflectance<sup>44</sup> and thermoreflectance<sup>45</sup> measurements were reported on this material below 4.5 and 3 eV, respectively, and room-temperature reflectivity<sup>46</sup> measurements were made below 12 eV. Our sample reflectivity is much higher at all corresponding energies than the measurements<sup>46</sup> reported previously, but peak positions are in reasonable agreement. In general, the interpretation of data below 6 eV must be based on the III-V analog GaAs.<sup>44, 45</sup> The similarity of the  $\text{ZnGeP}_2$  and

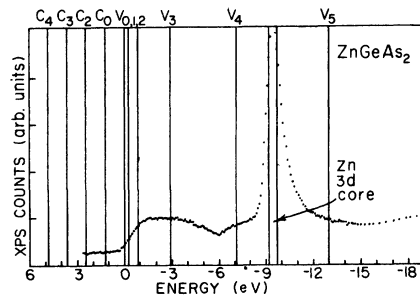


FIG. 11. XPS data for  $\text{ZnGeAs}_2$  with identified critical levels in the conduction and valence bands. The Zn  $3d$  core state is nearly degenerate with the As  $4s$  state which is roughly located near the energy labeled  $V_5$ .  $V_4$  labels states which are probably  $s$ -like around the cations. Conduction-band states are identified using transitions from the Zn  $3d$  core level.

$\text{ZnGeAs}_2$  reflectivity spectra above 8 eV and the similarity of the valence band XPS spectra for the two samples indicates that the final states for the observed transitions must be little affected by the substitution of arsenic for phosphorus even though the  $\text{ZnGeAs}_2$  and  $\text{ZnGeP}_2$  band gaps differ by 1.2 eV.

Figure 11 shows the deduced valence and conduction-band energies for  $\text{ZnGeAs}_2$  where critical transitions occur. These energies are consistent with both the XPS and reflectivity spectra. A meaningful, more detailed analysis can be made only when more accurate and complete energy band calculations become available.

#### ACKNOWLEDGMENTS

We wish to thank E. Rowe, C. H. Pruett, R. Otte, and the staff of the University of Wisconsin Physical Science Laboratory Synchrotron Radiation Center for providing a stable and intense vacuum-ultraviolet source. During the period of this research, the storage ring was operated with funds from AFOSR and later by NSF under operations Grant Nos. AFOSR-F44620-7-0-0029 and DMR-74-15089, respectively. The efforts of T. J. Moravec and K. K. Rao in developing the computer-controlled high-accuracy reflectometer are acknowledged along with the help of A. Prawirosusanto in sample preparation. We would also like to thank J. D. Wiley and J. L. Shay for their advice and help in obtaining the chalcopyrite specimens.

\*Present address: A-251, Physics Bldg., National Bureau of Standards, Washington, D. C. 20234.

<sup>1</sup>J. L. Shay and J. H. Wernick, *Ternary Chalcopyrite Semiconductors* (Pergamon, New York, 1975).

<sup>2</sup>A. Yu. Shileika, *Surf. Sci.* **37**, 730 (1973).

<sup>3</sup>M. Robbins, J. C. Phillips, and V. G. Lambrecht, Jr., *J. Phys. Chem. Solids* **34**, 1205 (1973).

<sup>4</sup>S. C. Abrahams and J. L. Bernstein, *J. Chem. Phys.* **59**, 5414 (1973).

<sup>5</sup>W. Gudat, E. E. Koch, P. Y. Yu, M. Cardona, and

- C. M. Penchina, *Phys. Status Solidi B* **52**, 505 (1972).
- <sup>6</sup>V. R. Sandrock and J. Treusch, *Z. Naturforsch. A* **19**, 844 (1964).
- <sup>7</sup>V. A. Chaldyshev and V. N. Pokrovskii, *Izv. Vyssh. Uchebn. Zaved. Fiz.* No. 2, 173 (1960); No. 5, 103 (1963).
- <sup>8</sup>C. V. de Alvarez, M. L. Cohen, A. E. Kohn, Y. Petroff, and Y. R. Shen, *Phys. Rev. B* **10**, 5175 (1974).
- <sup>9</sup>A. S. Poplavnoi, Yu. I. Polygalov, and V. A. Chaldyshev, *Soviet Physics Journal* **12**, No. 11, 1415 (1969) [*Izv. Vyssh. Uchebn. Zaved. Fiz.* No. 11, 58 (1969)].
- <sup>10</sup>A. S. Poplavnoi, Yu. I. Polygalov, and V. A. Chaldyshev, *Soviet Physics Journal* **13**, No. 6, 766 (1970); *ibid.* **13**, No. 7, 849 (1970). [*Izv. Vyssh. Uchebn. Zaved. Fiz.* No. 6, 95 (1970); *ibid.* No. 7, 17 (1970)].
- <sup>11</sup>A. S. Poplavnoi and Yu. I. Polygalov, *Soviet Physics Journal* **17**, No. 3, 354 (1974) [*Izv. Vyssh. Uchebn. Zaved. Fiz.* No. 3, 77 (1974)].
- <sup>12</sup>A. S. Poplavnoi and Yu. I. Polygalov, *Inorganic Materials* **7**, 1527 (1971); *ibid.* **7**, 1531 (1971) [*Izv. Akad. Nauk. SSR Neorg. Mater.* **7**, 1706 (1971); *ibid.* **7**, 1711 (1971)].
- <sup>13</sup>C. V. de Alvarez and M. L. Cohen, *Phys. Rev. Lett.* **30**, 979 (1973).
- <sup>14</sup>K. Kameswara Rao, T. J. Moravec, J. C. Rife, and R. N. Dexter, *Phys. Rev. B* **12**, 5937 (1975).
- <sup>15</sup>T. J. Moravec, J. C. Rife, and R. N. Dexter, *Phys. Rev. B* **13**, 3297 (1976).
- <sup>16</sup>"Syton" is a colloidal sol with a pH of 9–11. The SiO<sub>2</sub> particle size is about 1–2 μm. Manufactured by Monsanto Corp., St. Louis, Missouri.
- <sup>17</sup>J. L. Shay, B. Tell, H. M. Kasper, and L. M. Schiavone, *Phys. Rev. B* **7**, 4485 (1973).
- <sup>18</sup>P. W. Yu, W. J. Anderson, and Y. S. Park, *Solid State Commun.* **13**, 1883 (1973).
- <sup>19</sup>J. C. Rife, Ph.D. thesis (University of Wisconsin, 1976) (unpublished).
- <sup>20</sup>B. W. Veal and A. P. Paulikas, *Phys. Rev. B* **10**, 1280 (1974).
- <sup>21</sup>S. H. Wemple, J. D. Gabbe, and G. D. Boyd, *J. Appl. Phys.* **46**, 3597 (1975).
- <sup>22</sup>G. Martínez, M. Schlüter, M. L. Cohen, R. Pinchaux, P. Thiry, D. Dagneaux, and Y. Petroff, *Solid State Commun.* **17**, 5 (1975).
- <sup>23</sup>W. Braun, A. Goldmann, and M. Cardona, *Phys. Rev. B* **10**, 5069 (1974); W. Braun, thesis (Universität [TH] Karlsruhe, 1975) (unpublished).
- <sup>24</sup>B. Tell, J. L. Shay, and H. M. Kasper, *Phys. Rev. B* **4**, 2463 (1971).
- <sup>25</sup>R. L. Hengehold and F. L. Pedrotti, *J. Appl. Phys.* **46**, 5202 (1975).
- <sup>26</sup>J. Ringeissen, J. L. Regolini, and S. Lewonczuk, *Surf. Sci.* **37**, 777 (1973).
- <sup>27</sup>S. Kono and M. Okusawa, *J. Phys. Soc. Jpn.*, **37**, 1301 (1974).
- <sup>28</sup>This question is discussed in S. T. Pantelides, *Phys. Rev. B* **11**, 2391 (1975) and A. B. Kunz, *J. Phys. C* **7**, L231 (1974).
- <sup>29</sup>D. E. Aspnes, C. G. Olson, and D. W. Lynch, *Phys. Rev. B* **12**, 2527 (1975).
- <sup>30</sup>D. L. Greenaway and G. Harbeke, *Optical Properties and Band Structure of Semiconductors* (Pergamon, New York, 1968).
- <sup>31</sup>J. N. Gan, J. Tauc, V. G. Lambrecht, Jr., and M. Robbins, *Phys. Rev. B* **12**, 5797 (1975).
- <sup>32</sup>J. Gan, J. Tauc, V. G. Lambrecht, Jr., and M. Robbins, *Solid State Commun.* **15**, 605 (1974).
- <sup>33</sup>B. Tell and P. M. Bridenbaugh, *Phys. Rev. B* **12**, 3330 (1975).
- <sup>34</sup>John L. Freeouf, *Phys. Rev. B* **7**, 3810 (1973).
- <sup>35</sup>M. J. Luciano and C. J. Vesely, *Appl. Phys. Lett.* **23**, 453 (1973).
- <sup>36</sup>J. L. Shay and H. M. Kasper, *Phys. Rev. Lett.* **29**, 1162 (1972).
- <sup>37</sup>A. S. Poplavnoi, *Soviet Physics Journal* **11**, No. 9, 133 (1968) [*Izv. Vyssh. Uchebn. Zaved. Fiz.* No. 9, 142 (1968)].
- <sup>38</sup>F. Herman and S. Skillman, *Atomic Structure Calculations* (Prentice Hall, Englewood Cliffs, N.J., 1963).
- <sup>39</sup>C. V. de Alvarez, M. L. Cohen, L. Ley, S. P. Kowalczyk, F. R. McFeely, D. A. Shirley, and R. W. Grant, *Phys. Rev. B* **10**, 596 (1974).
- <sup>40</sup>A. Raudonis, V. S. Grigoreva, V. D. Prochukhan, and A. Šileika, *Phys. Status Solidi B* **57**, 415 (1973).
- <sup>41</sup>J. L. Shay, B. Tell, E. Buehler, and J. H. Wernick, *Phys. Rev. Lett.* **30**, 983 (1973).
- <sup>42</sup>M. L. Cohen and T. K. Bergstresser, *Phys. Rev.* **141**, 789 (1966).
- <sup>43</sup>Yu. F. Kavalayukas, A. V. Randonis, A. Yu. Shileika, A. S. Borschcherskii, and Yu. K. Undalov, *Sov. Phys.-Semicond.* **8**, 1008 (1975) [*Fiz. Tekh. Polnprov.* **8**, 1549 (1974)].
- <sup>44</sup>G. Z. Krivaite and A. Yu. Shileika, *Sov. Phys.-Semicond.* **7**, 1198 (1974) [*Fiz. Tekh. Polnprov.* **7**, 1796 (1973)].
- <sup>45</sup>C. C. Y. Kwan and J. C. Woolley, *Can. J. Phys.* **48**, 2085 (1970); *Phys. Status Solidi* **44**, K93 (1971); *Appl. Phys. Lett.* **18**, 520 (1971).
- <sup>46</sup>V. I. Donetskich, A. S. Poplavnoi, and V. V. Sobolev, *Phys. Status Solidi B* **48**, 541 (1971).